A EUROPEAN JOURNAL

CHEMPHYSCHEM

OF CHEMICAL PHYSICS AND PHYSICAL CHEMISTRY

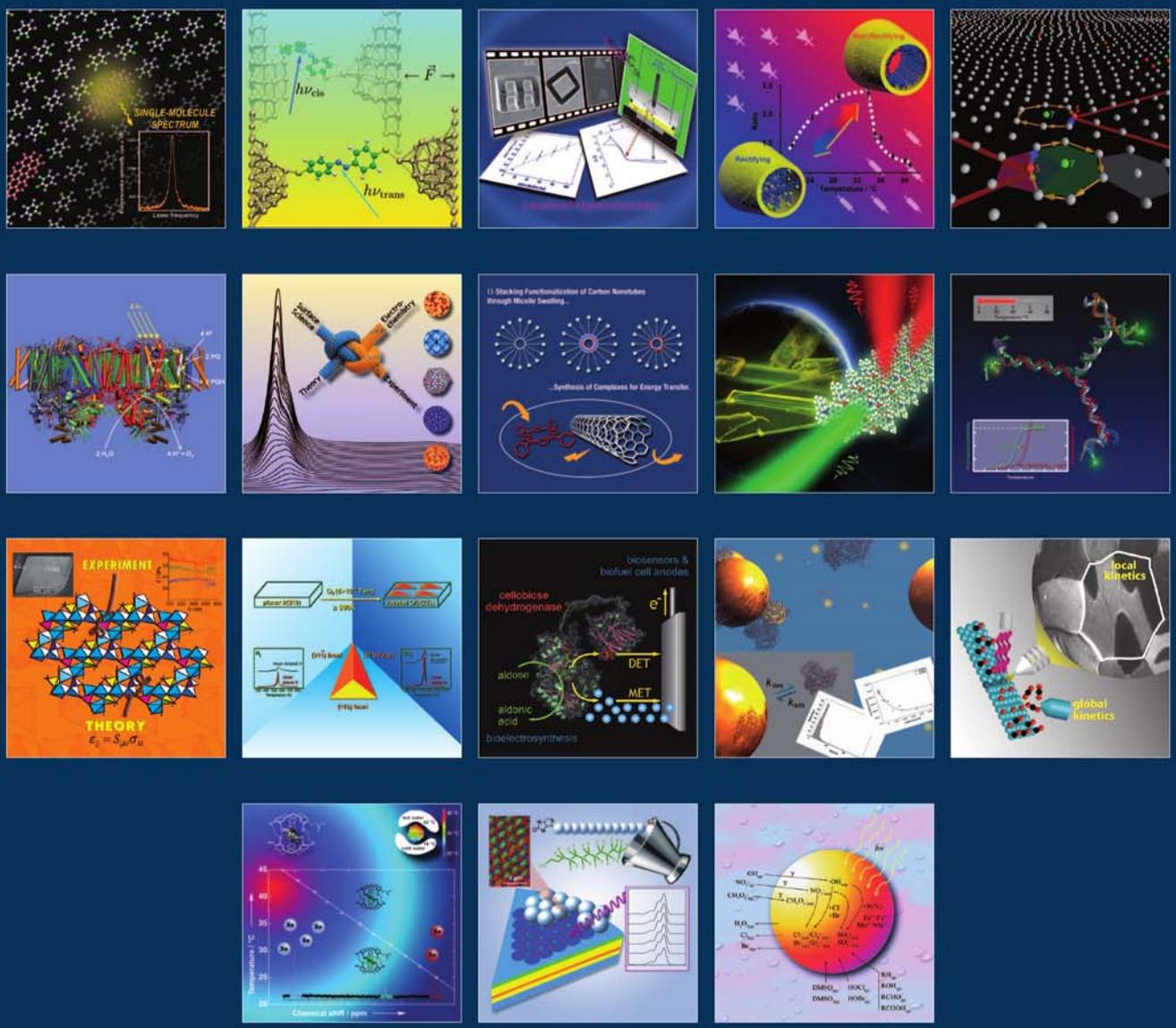

Reprint

ChemPubSoc Europe

WILEY-VCH

A EUROPEAN JOURNAL

CHEMPHYSCHEM

OF CHEMICAL PHYSICS AND PHYSICAL CHEMISTRY

Table of Contents

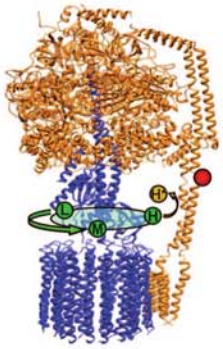

Molecular machines: H^+-ATP synthases couple transmembrane proton transport with ATP synthesis from ADP and inorganic phosphate by a rotational mechanism. Single-pair fluorescence resonance energy transfer (spFRET) in single molecules is a powerful tool to analyse conformational changes (see picture). It is used to investigate subunit movements in H^+-ATP synthases from *E. coli* (EF_0F_1) and from spinach chloroplasts (CF_0F_1) during catalysis.

WILEY-VCH

CHEMPHYSCHEM

DOI: 10.1002/cphc.201000921

Time-Dependent FRET with Single Enzymes: Domain Motions and Catalysis in H^+-ATP Synthases

Roland Bienert, Boris Zimmermann, Verena Rombach-Riegraf, and Peter Gräber *[a]

H^+-ATP synthases are molecular machines which couple transmembrane proton transport with ATP synthesis from ADP and inorganic phosphate by a rotational mechanism. Single-pair fluorescence resonance energy transfer (spFRET) in single molecules is a powerful tool to analyse conformational changes. It is used to investigate subunit movements in H^+-ATP synthases from *E. coli* (EF_0F_1) and from spinach chloroplasts (CF_0F_1) during catalysis. The enzymes are incorporated into liposome membranes, and this allows the generation of a transmembrane pH difference, which is necessary for ATP synthesis. After labelling of appropriate sites on different subunits with fluorescence donor and acceptor, the kinetics of spFRET are measured. Analysis of the E_{FRET} traces reveals rotational movement of the ε and γ subunits in 120° steps with opposite directions during ATP synthesis and ATP hydrolysis. The stepped movement is characterized by a 120° step faster than 1 ms followed by a rest period with an average dwell time of 15 ms, which is in accordance with the turnover time of the enzyme. In addition to the three conformational states during catalysis, also an inactive conformation is found, which is observed after catalysis.

1. Introduction

H^+-ATP synthases are important enzymes in the energy metabolism of all cells. They occur in the plasma membranes of bacteria, in the thylakoid membranes of chloroplasts and in the inner membranes of mitochondria. In these cell organelles electron transport (respiration or photosynthesis) generates a transmembrane electrochemical potential difference of protons. H^+-ATP synthases use the free energy released by the backflow of protons across the membrane to synthesize ATP from ADP and inorganic phosphate P_i ("chemiosmotic theory"[1]). As an example for their importance we consider the mitochondrial H^+-ATP synthases. Approximately 50 kg of ATP per day are synthesized in an average human, and its hydrolysis provides the energy for movement of muscles, ion transport, protein synthesis and so on.

H^+-ATP synthases are designated F_0F_1, since they consist of a hydrophilic F_1 part (subunits $\alpha_3\beta_3\gamma\delta\varepsilon$) containing three catalytic nucleotide and phosphate binding sites and a hydrophobic membrane-integrated F_0 part containing the proton binding sites (subunits ab_2c_{10}). For simplification, in the following the subunit composition and nomenclature of *E. coli* is used. The structure of F_0F_1 has been investigated by high-resolution electron microscopy[2,3] and X-ray crystallography (Figure 1).[4–6] The three-dimensional structure of EF_0F_1 obtained by electron microscopy is shown in the background; the F_1 part is located at the top, and the F_0 part, surrounded by detergent molecules, at the bottom, and the two parts are connected by a central stalk and a peripheral stalk.[3,7] The X-ray structures of mitochondrial F_1 and F_0F_1 have been the basis for calculation of an EF_0F_1 homology model of EF_0F_1[8] which is combined in Figure 1 with the results from electron microscopy. The F_1 part is formed by a barrel-like structure of alternating α and β subunits, and the γ subunit is located in the central cavity of this barrel. The central stalk is formed by the γ and ε subunits, and

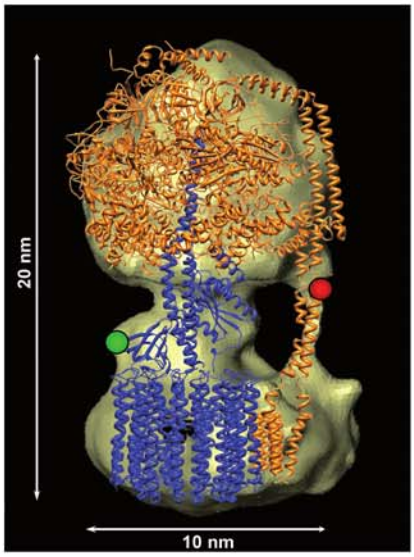

Figure 1. Side view of the homology model of the H^+-ATP synthase from *E. coli*. Rotor subunits are blue, and stator subunits orange. The donor position at ε56C is shown in green; the acceptor Cy5bis cross-links the two b subunits at position b64C and is shown in red. The three-dimensional structure of the enzyme obtained from electron microscopy data is shown as background. Unaccounted density in the F_0 part can be attributed to the detergent micelle shielding the hydrophobic part.

[a] *Dr. R. Bienert, Dr. B. Zimmermann, Dr. V. Rombach-Riegraf, Prof. Dr. P. Gräber*
Department of Physical Chemistry, University of Freiburg
Albertstrasse 23A, 79104 Freiburg (Germany)
Fax: (+49) 761-203-6189
E-mail: peter.graeber@physchem.uni-freiburg.de

both subunits are connected with the c_{10} ring in the membrane. The peripheral stalk, which is formed by the δ subunit (top of F_1), the two b subunits between F_0 and F_1 and the a subunit in the membrane, was not detected in the X-ray structure.[9]

The F_1 part contains three catalytic nucleotide binding sites on the β subunits, and the cooperation of the three catalytic sites is described by the "binding change theory".[10] According to this theory each catalytic site can adopt three conformational states ("loose" binding of ADP and P_i; "tight" formation of enzyme-bound ATP; "open" release of ATP), and at any moment each site is in a different conformational state. The centrally located γ subunit interacts differently with each αβ pair and induces thereby the three different conformations of the catalytic sites. Cooperation between the three sites is achieved by rotation of the γ subunit within the $\alpha_3\beta_3$ barrel, and this results in a simultaneous change of the conformations of all catalytic sites. The first high-resolution structure of the F_1 part corroborated this theory.[4] Rotation of the γ subunit within the F_1 part during ATP hydrolysis was observed by different methods, the most spectacular of which was visualization of this movement by video microscopy.[12–14]

Rotational movement is also carried out by the membrane-integrated c_{10} ring. Each c subunit carries a negatively charged amino acid in the middle of the membrane. This amino acid is protonated through a hydrophilic half-channel and it then moves into the hydrophobic membrane interior. After ten protonation steps it reaches an asymmetrically located exit channel, where the proton is released to the aqueous phase with low proton concentration. This mechanism of proton translocation leads to rotational movement of the c ring and, by interaction with the γ and the ε subunits, this rotation is transferred to the F_1 part.[15–20] Rotation of the c-subunit oligomer was observed during ATP hydrolysis with single immobilised F_0F_1 by video microscopy.[11,21–24] With respect to their function the subunits belong either to the stator part ($\alpha_3\beta_3\delta ab_2$, orange in Figure 1) or to the rotor part ($\gamma\varepsilon c_{10}$, blue in Figure 1).

First measurements of rotation of the γ subunit in single F_1 parts were carried out during ATP hydrolysis with immobilized F_1 parts by using either a fluorescent actin filament[12] or a gold bead[14] attached to the γ subunit as indicator. It was an unsolved question whether subunit rotation also occurs during proton transport coupled ATP synthesis. This requires, of course, the use of the holoenzyme (EF_0F_1) integrated into the membrane of a liposome. Such proteoliposomes allow a transmembrane ΔpH to be generated by an acid–base transition[25] in order to observe ATP synthesis.[26,27] Bulky indicators attached to the γ subunit, as used with immobilised F_1 parts, are not suitable for the holoenzyme because they sterically inhibit the rotation. Therefore, we chose single-pair fluorescence resonance energy transfer (spFRET) as an appropriate method.

Fluorescence resonance energy transfer (FRET) describes the transfer of excitation energy from a donor molecule to an acceptor molecule via a dipole–dipole interaction.[28] The FRET efficiency depends on the donor–acceptor distance according to Equation (1):

$$E_{FRET} = \frac{R_0^6}{R_0^6 + r_{DA}^6} = \frac{F_A}{F_A + \gamma F_D} \qquad \gamma = \frac{\eta_A \phi_A}{\eta_D \phi_D} \tag{1}$$

where D and A refer to donor and acceptor respectively, R_0 is the distance at which the transfer efficiency E_{FRET} is 50% and is called the Förster radius, r_{DA} the donor–acceptor distance, F_A and F_D are the fluorescence intensities, and γ is a correction factor containing the detection efficiency η and the quantum yield Φ. FRET can be used to measure donor–acceptor distances in the range between 1 and 8 nm. Since FRET is detectable at the single-molecule level,[29] it has been used in numerous applications to measure both inter- and intramolecular distances in biomolecules,[30–37] such as DNA–protein interactions[38,39] and dynamics within single enzymes.[40–43] To ensure single-molecule detection the probes are tethered to a surface,[44,45] confined in a liposome[46] or freely diffusing.[47]

Herein we focus on spFRET detection of freely diffusing H^+-ATP synthases incorporated into liposomes by confocal fluorescence microscopy. We give an overview of labelling strategies appropriate for multidomain enzymes such as the H^+-ATP synthases. Furthermore, we give a detailed setup description and analyse critical parameters such as observation time of freely diffusing particles and the number of fluorescence photons emitted by a single dye within a confocal volume. Finally, we present spFRET experiments with single H^+-ATP synthase during catalysis as well as considerations concerning spFRET data acquisition of intersubunit movements and data analysis.

2. The Biochemical System

The measurement of domain movements with spFRET requires the attachment of two fluorophores to appropriate sites of the enzyme.[48] Since we intend to measure relative subunit movements, one site must be on a rotor subunit, and the other on a stator subunit. Selective labelling (e.g., donor only on the rotor, acceptor only on the stator) requires either orthogonal functional groups of the fluorophores or a biochemical procedure which allows separate labelling of both sites with identically functionalised donor and acceptor. Usually, we use maleimide derivatives of cyanine dyes or ATTO dyes. Maleimide derivatives are especially useful for labelling proteins, since they react at pH 7 selectively with cysteine residues, which can be introduced genetically in EF_0F_1.

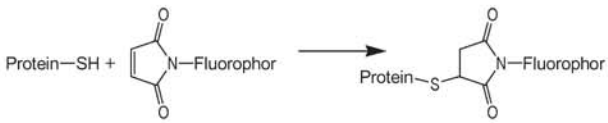

The proper sites are selected on the basis of the homology model shown in Figure 1. The b subunits of the peripheral stalk are suitable for labelling, since the fluorophores do not interfere with other subunits when they are attached to the region between F_1 and F_0. Since the homology model is highly speculative in this region, several stator mutants are generated (b40C, b51C, b53C, b62C, b64C).[49] As rotor mutants we use

γ107C, ε56C, and ε104C.[8,50] According to the homology model the distances between these cysteine residues on rotor and stator are between 4 and 8 nm. Such distances are well suited for FRET measurements.

In this Minireview only results with the mutants ε56C and b64C are described. However, this method was also used to measure the relative movements between other subunits in EF_0F_1[8,49–53] and in F_0F_1 from chloroplasts.[54] The procedure for selective labelling was as follows. First, F_1-ε56C was isolated and labelled with tetramethylrhodamine (TMR) as fluorescence donor. Then, F_0-b64C-F_1 was isolated and labelled with the acceptor Cy5.[49] Subunit b is a part of the peripheral stalk and it forms a dimer in F_0F_1, that is, the mutant enzyme contains two cysteine residues, and each of the b subunits may be labelled with a monofunctional Cy5. Therefore, there are two possible positions for the acceptor, and correspondingly two different donor–acceptor distances are obtained. To avoid these problems a dye with two maleimide groups (Cy5bis) was used.[8,50] This fluorophore cross-links the two b subunits and it has a well-defined position at the peripheral stalk (red circle in Figure 1). This acceptor-labelled F_0F_1 is integrated into the liposome membrane and the F_1 part is removed. In the last step the donor-labelled F_1 part is attached to the membrane-integrated F_0 part to give proteoliposomes in which donor and acceptor are each bound selectively to one subunit (see Figure 1).

To investigate the functional activity of the enzyme, the rate of ATP synthesis was measured after generation of a transmembrane electrochemical potential difference of protons by an acid–base transition (ΔpH and $\Delta\phi$). The rate of ATP synthesis of F_0-b64C-Cy5bis-F_1 was 75 s^{-1}. After removal of F_1 no ATP synthesis was detected. However, when the labelled F_1-ε56C-TMR was bound to the membrane-integrated F_0 part, a rate of 57 s^{-1} was observed. Obviously, reasonable catalytic activities are obtained after attachment of the fluorophores. From this rate, the mean turnover time was calculated and is 48 ms for synthesis of one ATP. Therefore, the conformational changes during catalysis are expected to occur in about 50 ms, that is, the turnover defines the time necessary in the FRET experiment.

3. The Confocal Set-Up

For investigation of the domain movements during catalysis a confocal setup was used (Figure 2). The sample is placed on a microscope slide. The intensity of the Nd:YAG laser (532 nm, 50 mW, Coherent) is attenuated to 100 μW, and the beam is focussed through a telescope and a water-immersion objective (UAPO 40×, N.A. 1.15, Olympus) into the centre of the sample. The fluorescence from the sample is collected by the same objective, passes through dichroic mirror 1 (dclp 545 nm, AHF) and is focussed on a pinhole (100 μm, OWIS). The superposition of the three-dimensional Gaussian intensity distribution of the laser (Figure 2 centre, green) and the ellipsoidal focus of the pinhole (yellow) forms the confocal volume. It is usually 10 fL and can be varied between 10 and 100 fL by using pinholes with different diameters. The confocal volume was determined by fluorescence correlation spectroscopy (FCS) with the diffusion coefficient of rhodamine 6G for calibration.[55]

Behind the pinhole the fluorescence is separated into the wavelength range of the donor (540–610 nm) and the acceptor (665–740 nm) by a second dichroic mirror (dcxr 630 nm, AHF) and appropriate interference filters (donor: HQ575/65, AHF and acceptor: 665lp, AHF). Fluorescence photons are detected with two avalanche photodiodes (APD, type SPCM-AQR-15, Perkin-Elmer). The fluorescence intensities of donor and acceptor (number of photons per time) are counted in parallel with a multichannel scaler (PMS 300, Becker & Hickl) and displayed as fluorescence time traces.

The efficiency of this setup can be estimated as follows. The laser beam has a photon flux of 3×10^{14} photons per second (power 100 μW, wavelength 532 nm). Beam focussing is diffrac-

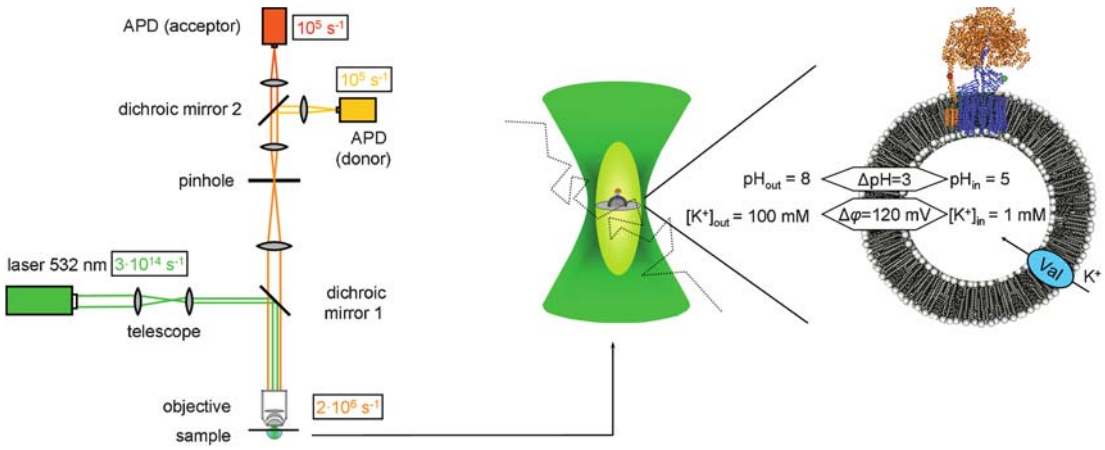

Figure 2. Scheme of single-pair FRET measurements. Left: Confocal set-up with simultaneous detection of donor and acceptor fluorescence (APD = avalanche photodiode). Centre: Three-dimensional intensity distribution of the focused laser beam (green). In the centre the focus of the pinhole is shown in yellow. The superposition of the laser focus and the pinhole focus defines the confocal volume (10×10^{-15} L). The grey circle shows the area of highest light intensity in the focus. The dotted line shows a diffusion trace of a F_0F_1 liposome through the confocal volume. Right: The liposome with the donor- (green) and acceptor-labelled (red) F_0F_1 is shown in an enlarged view. The magnitudes of the initial transmembrane ΔpH and $\Delta\phi$ are indicated.

tion-limited (see grey area in the centre of the confocal volume in Figure 2 centre). The radius of this area is given by the wavelength of the laser (532 nm), resulting in an area of 0.9×10^{-12} m^2 and a photon flux density of $I=3.5\times10^{26}$ m^{-2}s^{-1}. The number of photons absorbed by one fluorophore at this photon flux density can be estimated for ATTO532 (absorption coefficient $\varepsilon(532)=115\,000$ M^{-1}cm^{-1} = 11 500 m^{2}mol^{-1}) by Equation (2):

$$\frac{dN(abs)}{dt}=\frac{\varepsilon(532)}{N_A}\cdot I = \frac{11\,500\ m^2\,mol^{-1}\times 3.5\times10^{26}\ m^{-2}\,s^{-1}}{6\times10^{23}\ mol^{-1}}=6\times10^6\ s^{-1} \quad (2)$$

The number of emitted photons per time is obtained with the quantum yield $\Phi=0.4$ [Eq. (3)]:

$$\frac{dN(em)}{dt}=\Phi\frac{dN(abs)}{dt}=2.4\times10^6\ s^{-1} \quad (3)$$

Not all photons are collected by the objective, since fluorescence is emitted isotropically. In addition, photons are lost at the diverse optical components (dichroic mirrors, filters and APD). The overall detection efficiency (detected photons/emitted photons) of the set-up is estimated to be $D\approx0.08$, that is, the number of photons (sum of donor and acceptor photons) is given by Equation (4):

$$\frac{dN(detected)}{dt}=0.08\times2.4\times10^6\ s^{-1}\approx2\times10^5\ s^{-1} \quad (4)$$

To reduce the noise, photons are accumulated with a binning time of 1 ms. Therefore, if one fluorophore is in the confocal volume, a fluorescence intensity of 200 photons per millisecond is expected. This value is in good accordance with the experimental data (see Figure 4). A higher fluorescence intensity indicates that more than one fluorophore is present in the confocal volume.

The presence of only one FRET pair is achieved by adjusting the number of enzymes per liposome in the following way. The diameter of the liposomes is 150 nm, as determined by photon correlation spectroscopy. The sum of internal and external surface areas of the liposome is 1.3×10^5 nm^2 if we assume that the bilayer has a thickness of 8 nm. From the average area per lipid (0.6 nm^2),[56] the liposome contains 2.2×10^5 lipid molecules.[59] During reconstitution of EF_0F_1 a lipid concentration of 10.5 mM was used, and with the number of lipids per liposome a liposome concentration of 48 nM is calculated. During reconstitution the added EF_0F_1 concentration was less than 15 nM, and therefore we obtained a preparation in which only 25% of the liposomes contain an enzyme, and the other 75% contain no enzyme. The latter are not detected by fluorescence spectroscopy. The probability that two enzymes are reconstituted into one liposome is very low, and the presence of two labelled enzymes is detected by the doubled fluorescence intensity.

For spFRET measurements the EF_0F_1 liposomes are diluted to approximately 20 pM. The number of EF_0F_1 liposomes in the confocal volume (10 fL) is then $N=0.12$, that is, most of the time only background fluorescence is observed because there is no fluorophore in the confocal volume. It is a rare event that an enzyme enters and gives rise to a photon burst.

4. Single-Pair FRET during ATP Hydrolysis and Synthesis

To investigate the kinetics of subunit movements during catalysis, the average diffusion time of the proteoliposomes through the confocal volume must be adjusted in such a way that it is significantly longer than the turnover time of the chemical reaction. The turnover time of ATP synthesis is 50 ms and, correspondingly, the domain movements in the enzyme are expected to occur in the same time range. Therefore, the diffusion time through the confocal volume should be at least 50 ms. Figure 3 shows a measurement of the characteristic

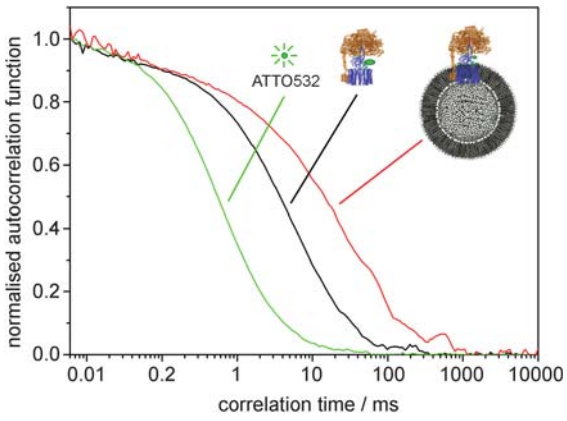

Figure 3. Normalised fluorescence autocorrelation curves of the fluorophore ATTO532 (green), F_0F_1-ATTO532 (black) and EF_0F_1-ATTO532 integrated in liposomes (red).

time for translational diffusion (τ_D) by fluorescence correlation spectroscopy. The free fluorophore ATTO532 (green, $\tau_D=4$ ms) and EF_0F_1-ATTO532 (black, $\tau_D=0.5$ ms) cannot be used for such measurements, since they diffuse too fast. The EF_0F_1 proteoliposomes (red) stay in the confocal volume for $\tau_D=20$ ms. Since this is a mean value, occasionally proteoliposomes have a diffusion time of up to a few hundred milliseconds, which is sufficient for measurements of domain movements during several turnovers.

Figure 4 shows spFRET measurements of domain movements. The proteoliposomes contain one donor- and acceptor-labelled EF_0F_1 and are diluted to 20 pM in a buffer. To investigate ATP synthesis, a transmembrane ΔpH of 3.0 and a transmembrane $\Delta\phi$ of 120 mV are generated by an acid–base transition, as shown schematically in Figure 2 (right). The proteoliposomes are equilibrated in an acidic buffer (pH 5) and then mixed rapidly with an alkaline buffer (pH 8) in a mixing chamber which is inserted into the microscope. Immediately after

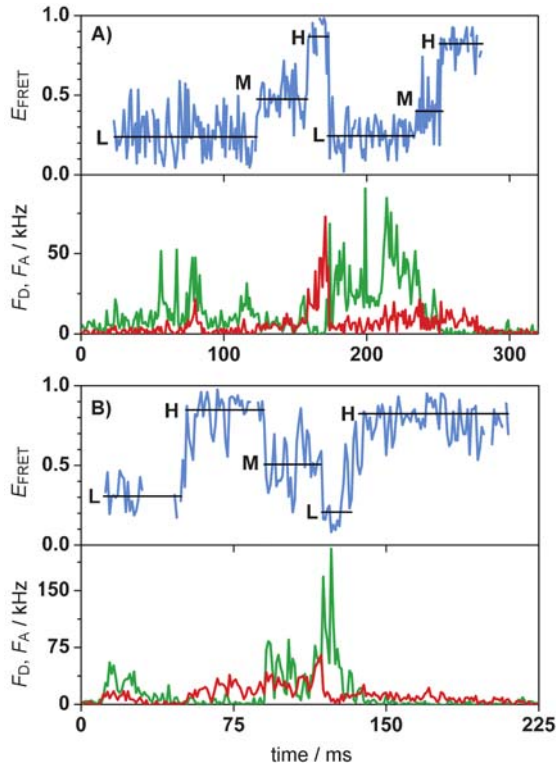

Figure 4. Photon bursts from donor- and acceptor-labelled F_0F_1 liposomes. Fluorescence intensity traces of donor (F_D, green) and acceptor (F_A, red) showing the diffusion of the liposome through the confocal volume. The FRET efficiency is calculated from these traces and is depicted in blue at the top. Three distinct levels (H, M and L) are observed. The black lines indicate the time average of each level. A) ATP hydrolysis showing the sequence of FRET states, L→H→M→L→H. B) ATP synthesis showing the opposite sequence of FRET states L→M→H→L→M→H.

mixing, fluorescence measurements are started. Since ΔpH decreases continuously after mixing, measurements are finished after one minute. When a proteoliposome enters the confocal volume the fluorescence of donor (green) and acceptor (red) increase from the background intensity (1 ms^{-1}) up to 50 ms^{-1} and both decrease again to the background when the proteoliposome leaves the confocal volume. Such an event is called a photon burst, and its frequency depends on the concentration of the proteoliposomes. The duration of the burst reflects the diffusion time of the proteoliposomes through the confocal volume (average 20 ms).The fluctuations of the fluorescence intensities result mainly from the light intensity distribution in the confocal volume. In addition to this effect alterations in fluorescence intensity can also be caused by intramolecular FRET changes. To extract the fluorescence changes due to FRET, the FRET efficiency E_{FRET} is calculated [see Eq. (1)]. The FRET efficiency does not depend on the location of the enzyme in the confocal volume; it only depends on the distance between donor and acceptor and their relative orientation.

Figure 4 shows two representative spFRET measurements of domain movements, one during ATP hydrolysis (Figure 4A) and one during ATP synthesis (Figure 4B). The FRET efficiencies are shown as blue traces, and the time averages of the FRET efficiencies as black lines. The E_{FRET} trace in Figure 4A indicates that in the first 100 ms the distance between the b and the ε subunits is large (low (L) FRET), at 120 ms it changes rapidly to a medium distance (medium (M) FRET), stays there for 40 ms and changes at 160 ms rapidly to a short distance (high (H) FRET). At 180 ms it changes again to the short distance and starts then with the same sequence.

The changes in FRET efficiency within single photon bursts are observed periodically with the sequences L–M–H during ATP synthesis (Figure 4B) and H–M–L during ATP hydrolysis (Figure 4A). Obviously, the direction of rotation depends on the direction of the chemical reaction. Surprisingly, the E_{FRET} traces in Figure 4 do not show a continuous but a stepped rotation: The rotor subunits ε and γ are docked to a specific αβ pair and remain there for some time (dwell time). Then, they move in less than 1 ms to the next αβ pair[60] and remain there until the next step occurs. This stepwise movement is characteristic and has been observed for all rotor subunits investigated so far.[8,49–51,54]

For further interpretation of single-molecule data a statistical analysis is required. Therefore, in each photon burst we identify regions of constant FRET efficiency (FRET state) and determine in those the mean FRET efficiency and the dwell time (see Figure 5A). The time averages of the FRET efficiencies are collected in Figure 5B. The histograms of FRET states during ATP hydrolysis and ATP synthesis reveal three peaks (L, M, H), which are fitted by Gaussian distributions. The maxima of the Gaussian distributions are taken as the ensemble mean FRET efficiencies of each population. These ensemble mean values and their standard deviations are converted to mean distances between the fluorophores attached to the amino acids ε56C and b64C, as shown in detail in reference [50] (see Table 1). To compare these data with the modified homology model, the program FRETsg[57] was used. Assuming a central axis of rotation and 120° steps, three positions of ε56C-TMR (green spheres, Figure 6A) are obtained and the distances to b64C-bisCy5 (red sphere, Figure 6A) are calculated. Comparison of experimental and theoretical data (see Table 1) shows that the ε subunit rotates in 120° steps relative to the b subunit (peripheral stalk). When viewed from the F_0 part to the F_1 part the rotation is clockwise during ATP synthesis (green arrow, Figure 6A) and anticlockwise during ATP hydrolysis, in accordance with earlier measurements with the immobilized F_1 part.[12] The equal areas below the three Gaussian distributions indicate that, during catalysis, each αβ pair is tagged by the rotor subunit with equal probability, as expected on basis of the binding change theory.[10] The same average distances (maxima of the distributions) are found for both directions of the reaction, that is, the reaction pathway seems to proceed via the same intermediates.

The distributions after catalysis differ in two respects. First, the maxima of the distributions are shifted to other distances, and therefore they are labelled L*, M*, H* in Figure 5B. Second, the histogram is strongly dominated by the H* state. In this state the enzyme is not catalytically active, that is, H* represents an inactive state. The distance between the ε and

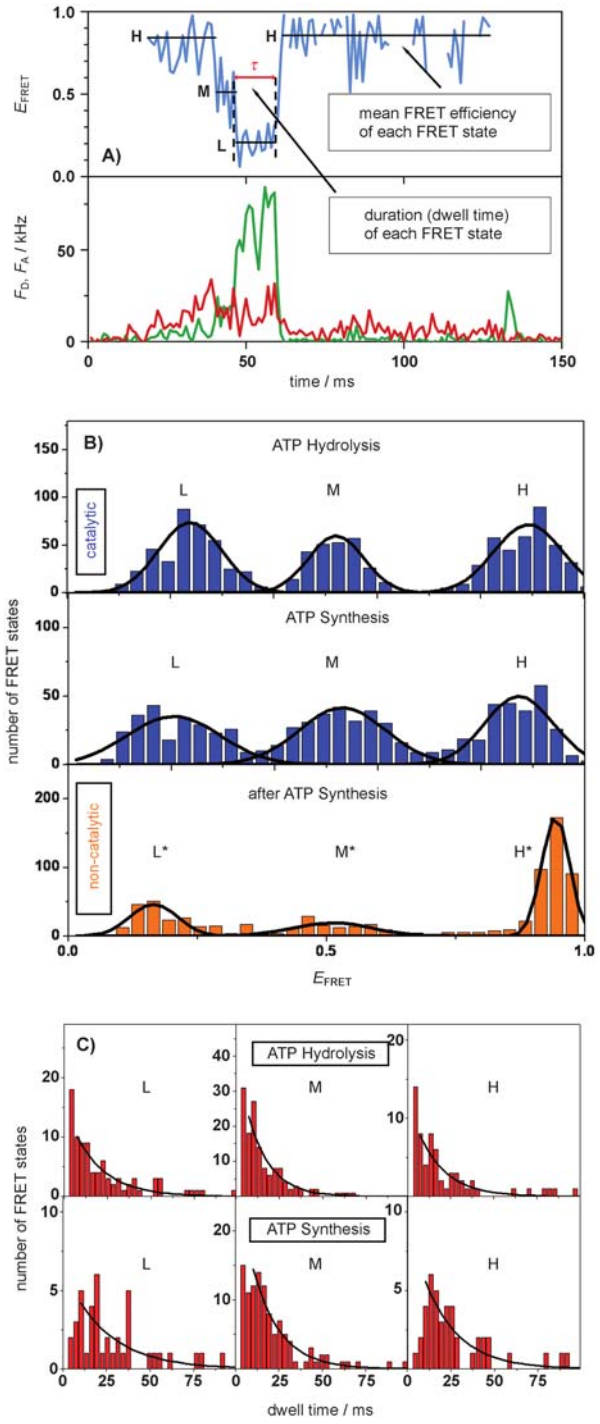

Figure 5. Analysis of E_{FRET} traces. A) The mean FRET efficiency (time average) indicating the mean donor–acceptor distance in one conformation (black horizontal line). The duration of a FRET state (τ, red) corresponds to the docking time of the $\gamma\varepsilon$ complex to one $\alpha\beta$ pair. B) Distribution of mean donor–acceptor distances in active enzymes during ATP synthesis and ATP hydrolysis (blue) and in inactive enzymes (orange). C) Distribution of the docking time of $\gamma\varepsilon$ to the three different $\alpha\beta$ pairs (L, M, H) during ATP synthesis and ATP hydrolysis.

the b subunits is shorter in this state than during catalysis. Figure 6A summarizes these results for EF_0F_1. The green arrow indicates the direction of rotation during ATP synthesis, and the yellow arrow shows inactivation of the enzyme.

Table 1. Mean FRET efficiencies, distances and dwell times under catalytic conditions.[50]

Condition	Mean FRET efficiency	Distance [nm] (FRET data)	Distance [nm] (homology model)	Dwell time [ms]
		ATP synthesis		
L	0.22 ± 0.09	7.8 ± 0.7	8.3	24.0 ± 4.4
M	0.53 ± 0.09	6.3 ± 0.4	5.1	15.4 ± 1.0
H	0.87 ± 0.07	4.6 ± 0.5	4.2	19.5 ± 2.2
		ATP hydrolysis		
L	0.24 ± 0.06	7.8 ± 0.7	8.3	17.6 ± 1.4
M	0.52 ± 0.06	6.3 ± 0.4	5.1	12.7 ± 1.0
H	0.89 ± 0.07	4.6 ± 0.5	4.2	15.8 ± 1.7
		After ATP synthesis		
H*	0.95 ± 0.03	4.0 ± 0.5	4.0	–

The dwell-time statistics are shown in Figure 5C. The average dwell time is 14 ms during ATP hydrolysis and 18 ms during ATP synthesis. In the M state the dwell time is lower and in the H and the L states it is higher than the average. This is a surprising observation. According to the binding change theory, all three catalytic sites are equal and carry out the same catalytic reaction. A possible explanation may be given by the asymmetry of the enzyme, that is, the interaction of one $\alpha\beta$ pair with the peripheral stalk could lead to subtle changes of the conformation of this $\alpha\beta$ pair, which might influence activation barriers of the catalytic reaction.

5. Rotation in Eukaryotic H^+-ATP Synthases

Almost all work on subunit rotation with single enzymes was carried out with bacterial enzymes.[8, 11, 12, 14, 20–24, 49–53] Recently, we were able to show subunit rotation in a eukaryotic H^+-ATP synthase.[54] Since in eukaryotic systems cysteine mutants are not easily available, it is challenging to find appropriate sites to attach the fluorophores. To label a subunit of the rotor complex, we used an endogenous cysteine residue of the γ subunit (γC322), where the donor (ATTO532) was covalently bound with high selectivity (Figure 6B, green sphere). For the stator a non-covalent labelling strategy was pursued. AMPPNP is a non-hydrolysable ATP analogue which binds with high affinity to ATP binding sites of CF_0F_1. The compound is commercially available as a fluorescent conjugate in which the acceptor fluorophore (ATTO655) is covalently bound to the ribose moiety. AMPPNP-ATTO655 was bound non-covalently at the non-catalytic site 4 on the α subunit (Figure 6B, red sphere).

Movement of the γ subunit relative to the α subunit during ATP synthesis within membrane-integrated CF_0F_1 was investigated with spFRET in the same way as described above for EF_0F_1. During ATP synthesis photon bursts with FRET transitions are observed. Three equally populated FRET states L, M and H are observed, which refer to active states of the enzyme. Without catalysis photon bursts show constant FRET efficiencies. Statistical analyses again reveal three FRET populations similar to those during catalysis and additionally a fourth population with a very high FRET efficiency. This population accumulates with time after catalysis, and we assume that this population

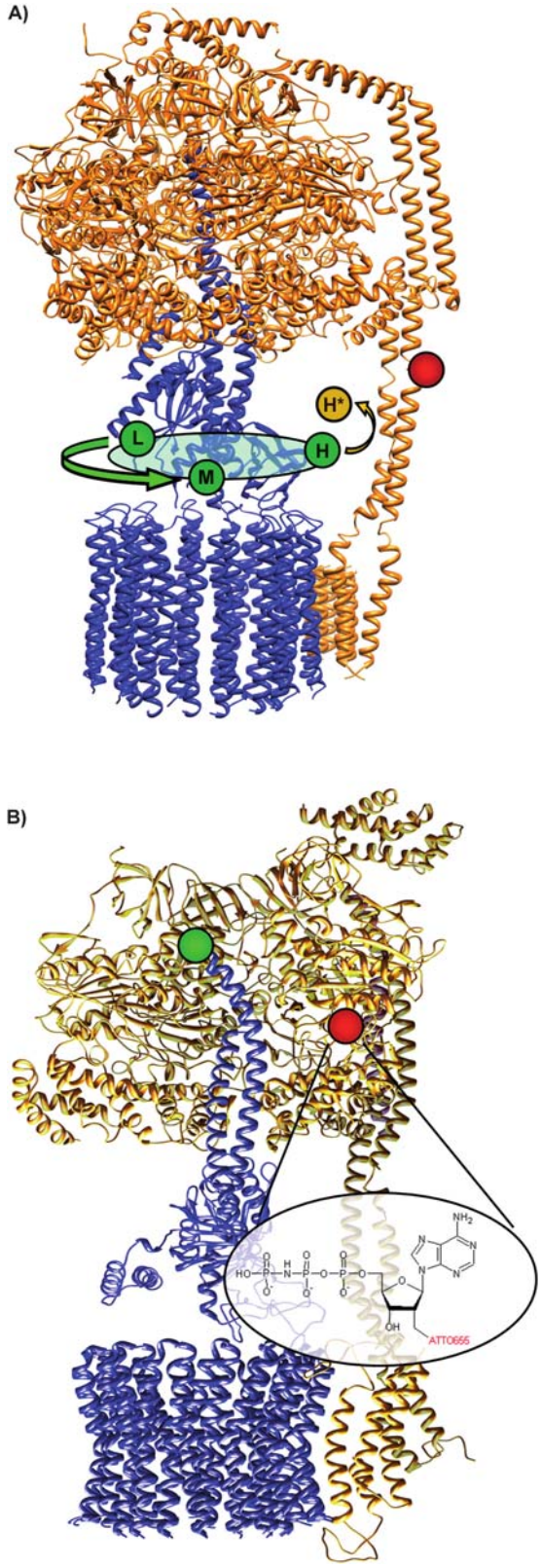

Figure 6. Homology models for EF_0F_1 and CF_0F_1. A) Model of movement of the ε subunit relative to the b subunit in EF_0F_1 during ATP synthesis (green arrow). The transition to the inactive state is indicated by a yellow arrow. B) Model of CF_0F_1. The donor (ATTO532, green sphere) is attached to γC322 and the acceptor (AMPPNP-ATTO655, red sphere) is bound to the non-catalytic nucleotide binding site 4.

represents an inactive state of the enzyme. Photon bursts in the presence of AMPPNP display no FRET transitions, since no catalysis is possible. Also in this case all enzymes are found in the same FRET state, with a high FRET efficiency. Thus, we have identified in addition to three active states two conformations of inactive CF_0F_1, one in the presence of ADP and one in the presence of AMPPNP.

6. Outlook

We used spFRET to analyse subunit movement in an enzyme which was integrated into the membrane of a liposome. The use of these proteoliposomes was necessary to generate transmembrane proton transport, which is part of the mechanism of the enzyme. In addition, the diameter of the liposomes can be varied to a certain extent, which allowed us to adjust the diffusion time of the proteoliposome through the confocal volume to the time range of the subunit movements.

Currently, we are investigating the possibility of improving the confocal set-up by addition of an optical trap. With such an arrangement it is possible to trap a proteoliposome in the confocal volume, and the observation time can be adjusted independently from the diffusion time. Another possibility is immobilisation of the proteoliposome at an appropriately coated glass surface and to use a total internal reflection fluorescence (TIRF) microscope for observation of FRET changes. Both approaches lead to a significant increase of the observation time. A longer time allows observation of several rotations of the enzyme. This is important to detect stepping of the c ring and its coupling to stepping of the γε complex. In addition, we expect to detect activation of the enzyme. This is a conformational change which occurs before the enzyme starts with rotation. A three-colour FRET[58] approach may be suitable in which one c subunit, one position of the γε complex and a reference position, such as the b subunits of the stator, are labelled, and the enzyme is investigated during ATP synthesis, immobilised either by surface tethering or in an optical trap.

Acknowledgements

We thank Dr. Michael Boersch for construction of the confocal setup and helpful discussions and Prof. Dr. C. A. M. Seidel for his help with the design of our confocal setup.

Keywords: enzyme catalysis · enzymes · FRET · molecular motions · single-molecule studies

[1] P. Mitchell, *Nature* **1961**, *191*, 144 – 148.
[2] S. Wilkens, R. A. Capaldi, *Biochim. Biophys. Acta Bioenerg.* **1998**, *1365*, 93 – 97.
[3] B. Böttcher, P. Gräber, *Biochim. Biophys. Acta Bioenerg.* **2000**, *1458*, 404 – 416.
[4] J. P. Abrahams, A. G. Leslie, R. Lutter, J. E. Walker, *Nature* **1994**, *370*, 621 – 628.
[5] D. Stock, A. G. W. Leslie, J. E. Walker, *Science* **1999**, *286*, 1700 – 1705.
[6] I. N. Watt, M. G. Montgomery, M. J. Runswick, A. G. W. Leslie, J. E. Walker, *Proc. Natl. Acad. Sci. USA* **2010**, *107*, 16823 – 16827.
[7] C. Mellwig, B. Böttcher, *J. Biol. Chem.* **2003**, *278*, 18544 – 18549.

[8] M. Diez, B. Zimmermann, M. Börsch, M. König, E. Schweinberger, S. Steigmiller, R. Reuter, S. Felekyan, V. Kudryavtsev, C. A. M. Seidel, P. Gräber, *Nat. Struct. Mol. Biol.* **2004**, *11*, 135 – 141.
[9] B. Böttcher, P. Gräber in *The Structure of the H^+-ATP Synthase from Chloroplasts* (Ed.: P. Fromme), Wiley-VCH, Weinheim, **2008**.
[10] P. D. Boyer, *Biochim. Biophys. Acta Bioenerg.* **1993**, *1140*, 215 – 250.
[11] M. Nakanishi-Matsui, M. Sekiya, R. K. Nakamoto, M. Futai, *Biochim. Biophys. Acta Bioenerg.* **2010**, *1797*, 1343 – 1352.
[12] H. Noji, R. Yasuda, M. Yoshida, K. Kinosita, Jr., *Nature* **1997**, *386*, 299 – 302.
[13] T. Hisabori, A. Kondoh, M. Yoshida, *FEBS Lett.* **1999**, *463*, 35 – 38.
[14] R. Yasuda, H. Noji, M. Yoshida, K. Kinosita, H. Itoh, *Nature* **2001**, *410*, 898 – 904.
[15] W. Junge, H. Lill, S. Engelbrecht, *Trends Biochem. Sci.* **1997**, *22*, 420 – 423.
[16] S. B. Vik, B. J. Antonio, *J. Biol. Chem.* **1994**, *269*, 30 364 – 30 369.
[17] P. Dimroth, *Biochim. Biophys. Acta Bioenerg.* **2000**, *1458*, 374 – 386.
[18] T. Elston, H. Y. Wang, G. Oster, *Nature* **1998**, *391*, 510 – 513.
[19] A. Aksimentiev, I. A. Balabin, R. H. Fillingame, K. Schulten, *Biophys J.* **2004**, *86*, 1332 – 1344.
[20] W. Junge, H. Sielaff, S. Engelbrecht, *Nature* **2009**, *459*, 364 – 370.
[21] Y. Sambongi, Y. Iko, M. Tanabe, H. Omote, A. Iwamoto-Kihara, I. Ueda, T. Yanagida, Y. Wada, M. Futai, *Science* **1999**, *286*, 1722 – 1724.
[22] H. Ueno, T. Suzuki, K. Kinosita, M. Yoshida, *Proc. Natl. Acad. Sci. USA* **2005**, *102*, 1333 – 1338.
[23] O. Pänke, K. Gumbiowski, W. Junge, S. Engelbrecht, *FEBS Lett.* **2000**, *472*, 34 – 38.
[24] R. Ishmukhametov, T. Hornung, D. Spetzler, W. D. Frasch, *EMBO J.* **2010**, *29*, 3911 – 3923.
[25] A. Jagendorf, E. Uribe, *Proc. Natl. Acad. Sci. USA* **1966**, *55*, 170 – 177.
[26] S. Fischer, C. Etzold, P. Turina, G. Deckers-Hebestreit, K. Altendorf, P. Gräber, *Eur. J. Biochem.* **1994**, *225*, 167 – 172.
[27] S. Fischer, P. Gräber, *FEBS Lett.* **1999**, *457*, 327 – 332.
[28] T. Förster, *Ann. Phys.* **1948**, *437*, 55 – 75.
[29] T. Ha, T. Enderle, D. F. Ogletree, D. S. Chemla, P. R. Selvin, S. Weiss, *Proc. Natl. Acad. Sci. USA* **1996**, *93*, 6264 – 6268.
[30] S. Weiss, *Nat. Struct. Biol.* **2000**, *7*, 724 – 729.
[31] A. N. Kapanidis, T. Strick, *Trends Biochem. Sci.* **2009**, *34*, 234 – 243.
[32] R. B. Zhou, M. Schlierf, T. Ha, *Methods Enzymol.* **2010**, *475*, 405 – 426.
[33] C. Joo, H. Balci, Y. Ishitsuka, C. Buranachai, T. Ha, *Annu. Rev. Biochem.* **2008**, *77*, 51 – 76.
[34] K. Henzler-Wildman, D. Kern, *Nature* **2007**, *450*, 964 – 972.
[35] T. Ha, *Methods* **2001**, *25*, 78 – 86.
[36] R. D. Smiley, G. G. Hammes, *Chem. Rev.* **2006**, *106*, 3080 – 3094.
[37] R. Roy, S. Hohng, T. Ha, *Nat. Methods* **2008**, *5*, 507 – 516.
[38] T. Ha, I. Rasnik, W. Cheng, H. P. Babcock, G. H. Gauss, T. M. Lohman, S. Chu, *Nature* **2002**, *419*, 638 – 641.
[39] S. Myong, I. Rasnik, C. Joo, T. M. Lohman, T. Ha, *Nature* **2005**, *437*, 1321 – 1325.
[40] M. Margittai, J. Widengren, E. Schweinberger, G. F. Schröder, S. Felekyan, E. Haustein, M. Konig, D. Fasshauer, H. Grubmüller, R. Jahn, C. A. M. Seidel, *Proc. Natl. Acad. Sci. USA* **2003**, *100*, 15516 – 15521.
[41] B. Schuler, E. A. Lipman, W. A. Eaton, *Nature* **2002**, *419*, 743 – 747.
[42] B. Schuler, W. A. Eaton, *Curr. Opin. Struct. Biol.* **2008**, *18*, 16 – 26.
[43] Y. Ishii, T. Yoshida, T. Funatsu, T. Wazawa, T. Yanagida, *Chem. Phys.* **1999**, *247*, 163 – 173.
[44] X. W. Zhuang, L. E. Bartley, H. P. Babcock, R. Russell, T. J. Ha, D. Herschlag, S. Chu, *Science* **2000**, *288*, 2048 – 2051.
[45] S. A. McKinney, A. C. Declais, D. M. J. Lilley, T. Ha, *Nat. Struct. Biol.* **2002**, *10*, 93 – 97.
[46] I. Cisse, B. Okumus, C. Joo, T. J. Ha, *Proc. Natl. Acad. Sci. USA* **2007**, *104*, 12646 – 12650.
[47] A. A. Deniz, M. Dahan, J. R. Grunwell, T. J. Ha, A. E. Faulhaber, D. S. Chemla, S. Weiss, P. G. Schultz, *Proc. Natl. Acad. Sci. USA* **1999**, *96*, 3670 – 3675.
[48] L. Stryer, R. P. Haugland, *Proc. Natl. Acad. Sci. USA* **1967**, *58*, 719 – 726.
[49] M. Börsch, M. Diez, B. Zimmermann, R. Reuter, P. Gräber, *FEBS Lett.* **2002**, *527*, 147 – 152.
[50] B. Zimmermann, M. Diez, N. Zarrabi, P. Gräber, M. Börsch, *EMBO J.* **2005**, *24*, 2053 – 2063.
[51] M. G. Düser, N. Zarrabi, D. J. Cipriano, S. Ernst, G. D. Glick, S. D. Dunn, M. Börsch, *EMBO J.* **2009**, *28*, 2689 – 2696.
[52] E. Galvez, M. Düser, M. Börsch, J. Wrachtrup, P. Gräber, *Biochem. Soc. Trans.* **2008**, *36*, 1017 – 1021.
[53] S. Steigmiller, B. Zimmermann, M. Diez, M. Börsch, P. Gräber, *Bioelectrochemistry* **2004**, *63*, 79 – 85.
[54] R. Bienert, V. Rombach-Riegraf, M. Diez, P. Gräber, *J. Biol. Chem.* **2009**, *284*, 36240 – 36247.
[55] J. Widengren, U. Mets, R. Rigler, *J. Phys. Chem.* **1995**, *99*, 13368 – 13379.
[56] J. F. Nagle, R. T. Zhang, S. Tristram-Nagle, W. J. Sun, H. I. Petrache, R. M. Suter, *Biophys. J.* **1996**, *70*, 1419 – 1431.
[57] G. F. Schröder, H. Grubmüller, *J. Chem. Phys.* **2003**, *119*, 9920 – 9924.
[58] S. Hohng, C. Joo, T. Ha, *Biophys. J.* **2004**, *87*, 1328 – 1337.
[59] K. Förster, P. Turina, F. Drepper, W. Haehnel, S. Fischer, P. Gräber, J. Petersen, *Bba-Bioenergetics* **2010**, *1797*, 1828 – 1837.
[60] B. Zimmermann, M. Diez, M. Börsch, P. Gräber, *Bba-Bioenergetics* **2006**, *1757*, 311 – 319.

Received: November 4, 2010
Published online on February 2, 2011

